Preprint Title Interaction of Small Biothiols with Silver and Gold Nanoparticles

Authors Barbara Pem, Igor M. Pongrac, Lea Ulm, Ivan Pavičić, Valerije Vrček, Darija Domazet Jurašin, Marija Ljubojević, Adela Krivohlavek and Ivana Vinković Vrček

Article Type Full Research Paper

Supporting Information File 1 Supporting Information BJN_VinkovicVrcek.docx; 665.3 KB

ORCID® iDs Barbara Pem - https://orcid.org/0000-0001-9631-8985; Valerije Vrček - https://orcid.org/0000-0003-1624-8126; Ivana Vinković Vrček - https://orcid.org/0000-0003-1382-5581

Interaction of Small Biothiols with Silver and Gold Nanoparticles

Barbara Pem[1], Igor M. Pongrac[2], Lea Ulm[3], Ivan Pavičić[1], Valerije Vrček[4], Darija Domazet Jurašin[5], Marija Ljubojević[1], Adela Krivohlavek[3], Ivana Vinković Vrček[1,]*

[1] Institute for Medical Research and Occupational Health, Ksaverska cesta 2, 10000 Zagreb, Croatia

E-mail: ivinkovic@imi.hr

[2] University of Zagreb, School of Medicine, Croatian Institute for Brain Research, Šalata 12, 10000 Zagreb, Croatia

[3] Andrija Štampar Teaching Institute of Public Health, Mirogojska 16, 10000 Zagreb, Croatia

[4] Faculty of Pharmacy and Biochemistry, University of Zagreb, Ante Kovačića 1, 10000 Zagreb, Croatia

[5] Rudjer Boskovic Institute, Bijenička cesta 54, 10000 Zagreb, Croatia

[*] Corresponding author: e-mail: ivinkovic@imi.hr

Graphical abstract

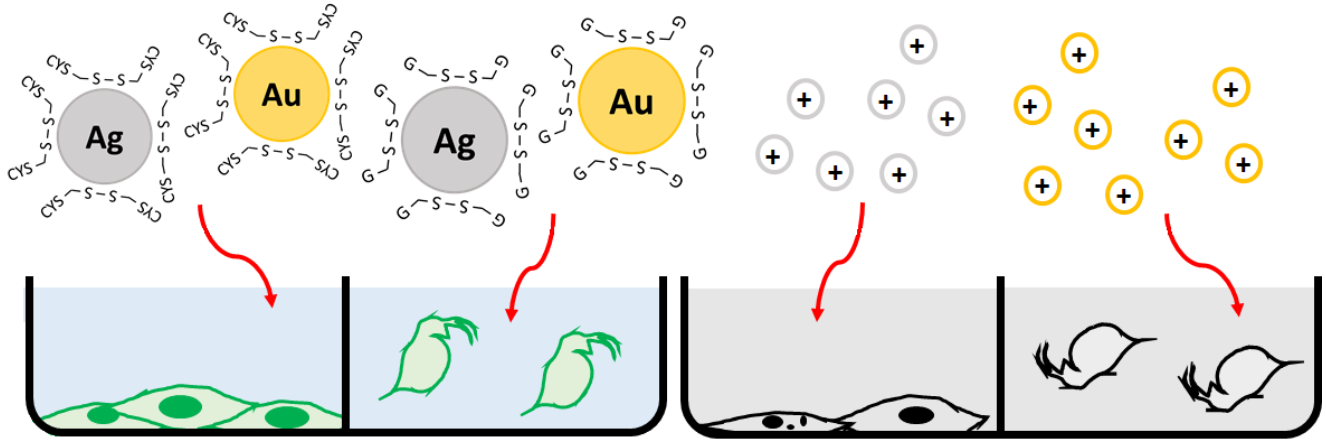

Abstract

Improvement in nanosafety is one of the major tasks for innovation force of nanotechology, which may be accomplished by design and development of biocompatible nanomaterials. Biocompatibility assessment demands investigation of nano-bio interactions that affect behavior and fate of nanoparticles in biological systems. Metallic nanoparticles (NPs) are particularly prone to interact with endogenous biothiols like cysteine and glutathione. This study was designed to evaluate intimate interactions between cysteine and glutathione with biomedically relevant metallic NPs, i.e. silver (AgNPs) and gold (AuNPs). Systematic and comprehensive analysis revealed that preparation of AgNPs and AuNPs in the presence of biothiols lead to stable NPs stabilized with oxidized forms of biothiols. Their biocompatibility was tested by evaluation of cell viability, ROS production, apoptosis induction and DNA damage in murine fibroblast cells (L929), while ecotoxicity was tested using aquatic model organism *Daphnia magna*. The toxicity of these NPs was considerably lower compared to the ionic metal forms. Comparison with data published on polymer-coated NPs evidenced that surface modification with biothiols made them safer for the environment, but more toxic for use in humans. These results represent significant contribution to the collection of knowledge on the role of biothiols on the fate and behavior of metal-based nanomaterials.

Keywords: nano-bio interactions, cysteine, glutathione, biocompatibility, ecotoxicity

INTRODUCTION

Metallic nanoparticles (NPs) like silver and gold have been employed in a wide range of products and application including different biomedical field owing to their remarkable physico-chemical properties. Silver nanoparticles (AgNPs) are thus extensively used in antimicrobial coatings for medical devices, wound dressing, cosmetic products and food packaging due to their antimicrobial, antiangiogenic and anti-inflammatory activities.[1–5] Biomedical application of gold nanoparticles (AuNPs) ranges from molecular imaging, targeted drug delivery, gene therapy, cancer treatment or radiosensitization and theranostics.[1,4,6] Moreover, AgNPs and AuNPs are among the most investigated engineered nanomaterials for medical uses. A search performed in the Web of Science (WoS) database on November 11th 2018 using the search terms "nano*" and "medic*" yielded a total of 63032 papers. Out of those, silver was reported in 6004 papers (9.5%) and gold 8757 (13.9%) revealing that these two NPs types alone are represented by almost one quarter of all published studies on biomedical aspects of NPs (**Figure S1 in Supporting Information (SI)**). In hand with the rise of papers reporting development of NPs for biomedical uses, WoS search showed that there are ample studies on toxicity effects of AgNPs and AuNPs *in vitro* and *in vivo*. There are a number of studies representing that AgNPs negatively impact cell membranes, interfere with signaling pathways, disrupt the cell cycle, cause mitochondrial dysfunction, oxidative stress, DNA damage and apoptosis.[7–9] Many reports on AgNPs toxicity attribute it fully or partially to dissolved or released ionic silver.[10–16] Dissolution of AgNPs in both biological and different environmental media has been proven, although the rate and amount varies depending on the AgNPs characteristics determined by the size, stabilization and the presence of other molecules.[17] Still, some studies have discussed that AgNPs toxicity cannot be

explained solely by the release of Ag^+ ions in the system.[18,19] Studies on AuNPs toxicity provide conflicting results, with some authors claiming no toxicity was found,[20–25] while others reported adverse effects caused by AuNPs.[26–32] Most likely mechanism of their toxicity is generation of reactive oxygen species (ROS) and reactive nitrogen species (RNS) that trigger necrosis or apoptosis.[33] So far, general consensus regarding NPs toxicity is that their toxic effects cannot be conclusively defined, as mechanism of their action depends on their physico-chemical properties (shape, size, charge, coating agents), but also on targeted cells, tissues and/or organisms as well as on the type of testing itself.[34–38] Therefore, each individual NP type must be tested on various cell cultures using standardized and reliable assay protocols to adequately assess and explain effects.[39] Anyhow, exposure to NPs may lead to their uptake, translocation, and most likely biotransformation within the body.

It has been demonstrated that AgNPs and AuNPs can be absorbed into systemic circulation via different routes.[40–43] Absorbed or intravenously applied NPs will accumulate in different body compartments.[44–46] It has also been demonstrated that AgNPs are prone to oxidative dissolution in biological media and the released Ag^+ reacts with thiolate groups of sulfur-containing biomolecules,[47] which may lead to the formation of thiol-coated AgNPs.[48] In addition, new clusters consisting of Ag_2S can be created from free Ag^+.[47] This process, known as sulphidation, affects AgNPs behavior in the biological system,[49] most notably reducing their toxicity.[47,50] The binding of thiols to AuNP surface has also been well investigated.[51–54] As the most abundant intracellular biothiols are cysteine (CYS) and glutathione (GSH), their role in intracellular sulphidation and/or adsorption on the surface of NPs should be considered during evaluation of efficacy, safety and behavior of AgNPs and AuNPs *in vivo*.[47,55] Due to many existing knowledge gaps in this field, there is a need for additional data on nano-bio interface formed after metal-based NPs reach biological environment. The WoS search

resulted in less than 5% of papers providing results on the nano-bio interface between biothiols and AgNPs or AuNPs (**Figure S1 in SI**).

To gain further insight into the effect of biothiols on biocompatibility or toxicity of bioactive metallic NPs, this study comprehensively investigated mechanism of formation of AgNPs and AuNPs in the presence of CYS and GSH and their subsequent biological effects. Murine fibroblasts were used as cell model to study mammalian toxicity, while *Daphnia magna* was the representative aquatic organism to evaluate ecotoxicity. Contrasting the safety levels of biothiol-coated NPs with metal ions, this study aimed to gain insight into the possible reduction or enhancement of toxicity of AgNPs and AuNPs after interaction with CYS and GSH following biotransformation. Obtained results provide additional insights to elucidate possible scenarios of AgNPs and AuNPs biological fate.

RESULTS AND DISCUSSION

Synthesis and characterization of nanoparticles

For the AgNPs and AuNPs synthesis, common bottom-up approach was applied using sodium borohydride as agent to reduce Ag^{+} and Au^{3+}, respectively. Optimization of synthetic protocol was achieved by a series of experiments in which the reaction conditions (i.e. temperature, mixing time and rate, concentration of reactants) were carefully tested in order to obtain small, spherical and stable NPs. Molar ratio of reactants [metallic salts]:[$NaBH_4$]:[biothiol] varied as summarized in **Tables S1 and S2 of SI**. The particles were deemed unstable if they fully precipitated after synthesis and could not be re-dispersed, otherwise they were noted as stable. After each synthesis, careful characterization of stable NPs was performed by DLS, ELS and TEM techniques. Obtained results showed that molar ratio of reactants was more important for successful preparation of stable NPs than all other parameters and experimental conditions. With regard to the CYS as stabilizing agent, results indicated that its molar concentration should be ca. ten times lower than concentration of $NaBH_4$, while GSH allowed much

wider concentration ranges. In the case of molar ratio reducing agent vs. metallic salts, larger excess of $NaBH_4$ (> 5 times) was needed to obtain stable NPs. Finally, we have selected molar ratio [metallic salts]:[$NaBH_4$]:[biothiol] = 1:10:1 for further work as it gained favorable NP size (~ 10 nm) and long term stability.

NMR is an excellent tool to determine the interactions of small organic molecules with metallic NPs because the small changes in the chemical environment result in chemical shifts in NMR spectra. Several studies have been published that confirm the validity of this technique in establishing thiol-NP interactions.[51,56–58]

In a typical experiment, the mixture of metallic salt ($HAuCl_4$ or $AgNO_3$), $NaBH_4$, and CYS (as described above) was stirred under argon in the ultrapure water at room temperature for 90 minutes. The progress of the reaction was monitored by ^{1}H NMR spectroscopy. The aliquots were taken from the reaction mixture at selected time points and D_2O was added (or a D_2O-filled capillary was used for a lock signal). Along with the disappearance of ^{1}H NMR signals of the reactant (CYS), a new set of proton signals of the product emerged (**Figure 1**). All new signals were shifted downfield by ca. 0.2 ppm. According to detailed ^{1}H and ^{13}C NMR analysis (see **Figures S2-S4 in SI**), we conclude that the cystine was formed.

After completion (no CYS signals existed in ^{1}H NMR spectrum) the remaining signals were broadened in time, which indicates the cystine binding to the NP surface. It is well known that ^{1}H NMR signals from ligands bound to NPs display broad line widths.[59–61]

Exactly the same ^{1}H NMR profile was recorded for the reaction mixture which consisted of cysteine and $NaBH_4$, i.e. no metallic salt was added (see **Figure S4 in SI**). This means that, during the regular procedure for the cysteine-coated NPs synthesis (as described elsewhere), the cystine may be formed prior to its binding to the NP surface. It was shown earlier that cysteine in the reaction with metallic salt ($HAuCl_4$) underwent dimerization to form cystine.[62] However, no NMR evidence for that was

provided. In our case, the dimerization occurred in the reaction mixture consisting of $NaBH_4$ and cysteine. It is possible that some $NaBH_4$ hydrolysis products[63–65] induce this dimerization, but the detailed mechanism underlying the reaction is out of the scope of this paper.

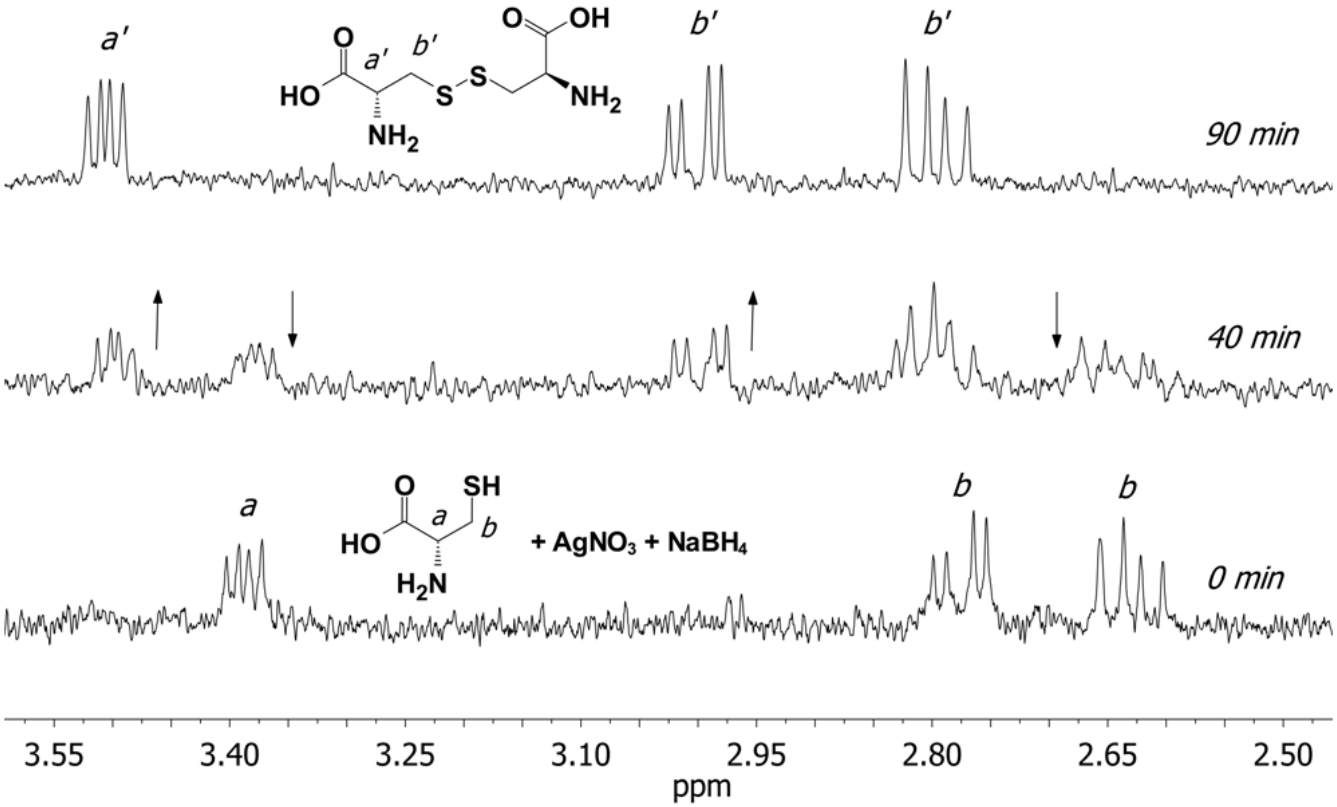

Figure 1. ^1H NMR spectra of the reaction mixture aliquots (5.6 mM cysteine, 56 mM $NaBH_4$, and 5.6 mM $AgNO_3$, in ultrapure water/D_2O added) taken at several time points. The arrows show how proton signals (for cysteine and cystine) change with time.

The very similar was observed in the case of GSH which undergoes dimerization to GSSG in the presence of Au^{3+} (or Ag^+) salt and $NaBH_4$ (a standard protocol for the NPs synthesis) (**Figure 2**), or in the presence of $NaBH_4$ alone (see **Figure S5 in SI**). In conclusion, this indicates that both biothiols

(GSH and CYS) bind to the NP surfaces in their oxidized form, which expands some earlier proposals.[51,66]

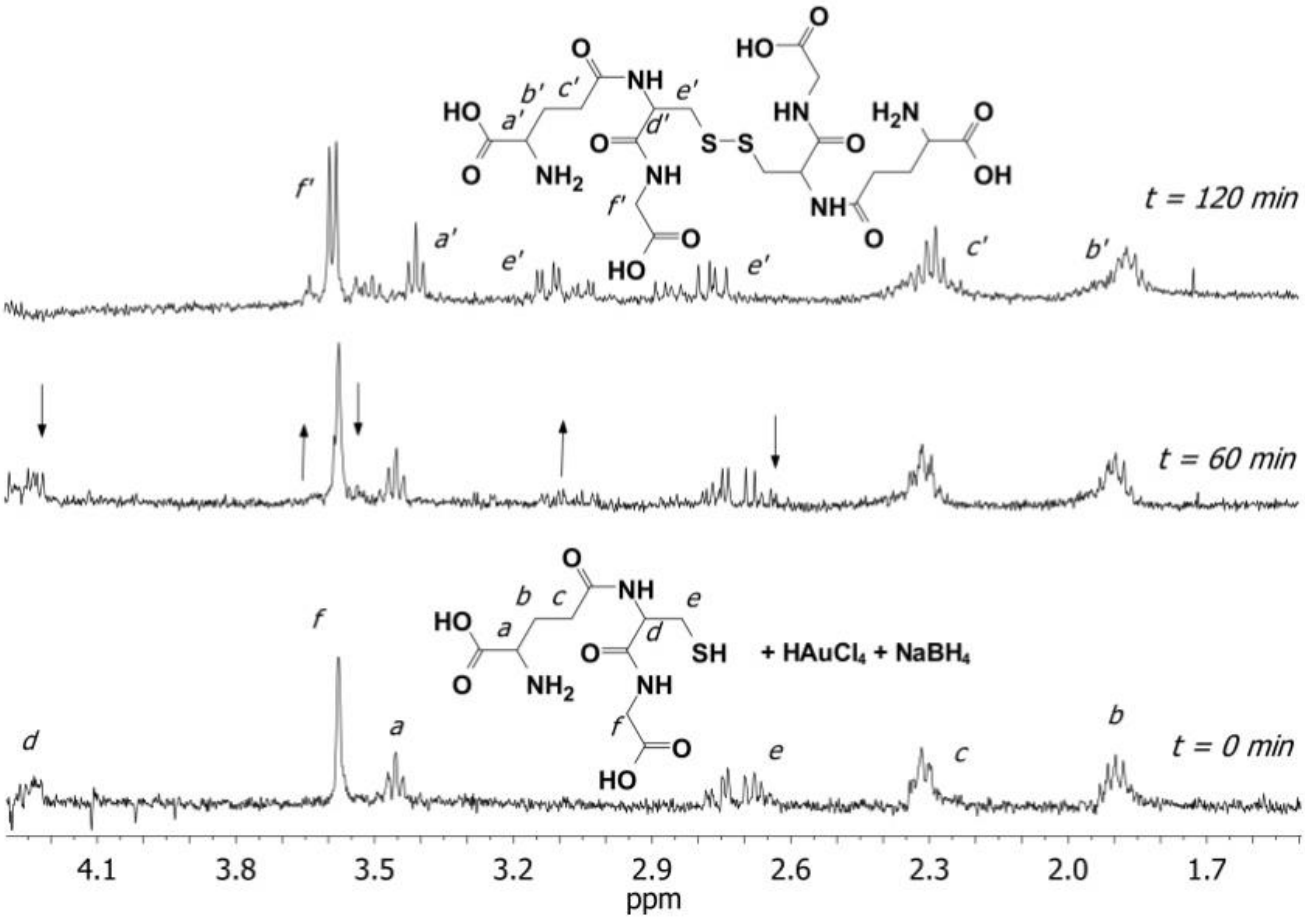

Figure 3. ^{1}H NMR spectra of the reaction mixture aliquots (5.6 mM glutathione, 56 mM $NaBH_4$, and 5.6 mM $HAuCl_4$, in ultrapure water/D_2O added) taken at several time points. The arrows show how proton signals (for GSH and GSSG) change with time.

Detailed characterization of prepared NPs dispersed in the UPW revealed negative surface charge. Observed ζ potential values (**Table 1**) were indicative for high NPs stability, as the NPs are generally considered electrostatically stabilized when the absolute values of ζ potential exceed 30 mV.[67] Size

distribution of all NPs was bimodal, while AgNPs were generally smaller than AuNPs (Table 1). TEM experiments showed spherical shape for all NPs (**Figure 3**).

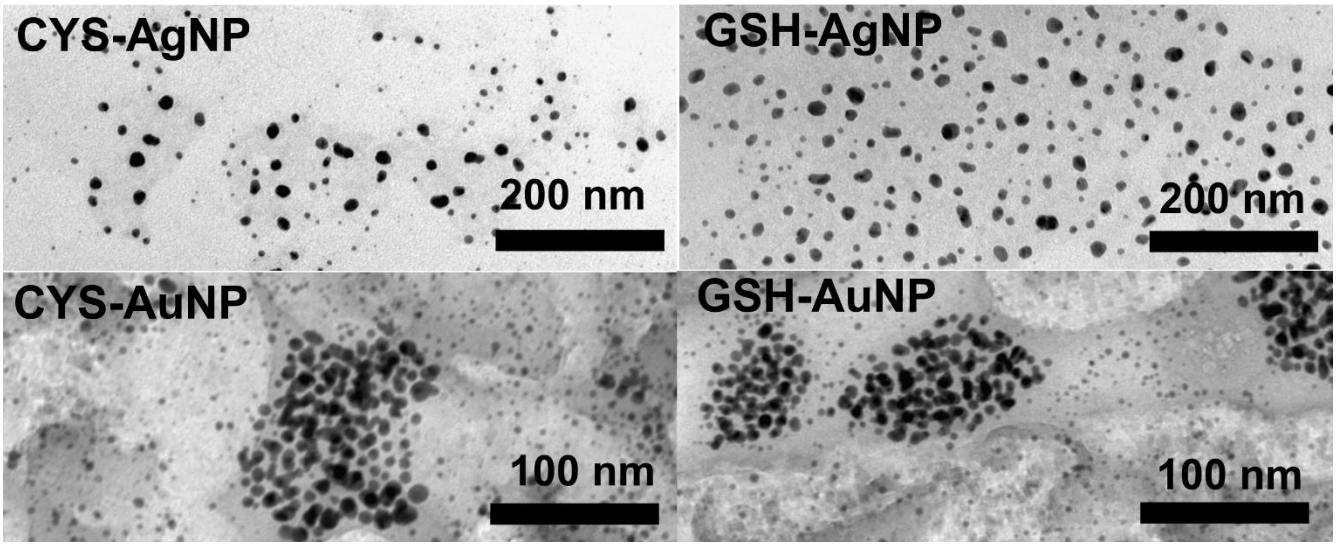

Figure 3. Transmission electron micrographs of silver (AgNPs) and gold nanoparticles (AuNPs) prepared in the presence of cysteine (CYS) or glutathione (GSH).

Table 1. Hydrodynamic diameter (d_H) and zeta potential (ζ) of silver (AgNPs) and gold nanoparticles (AuNPs) stabilized with cysteine (CYS) or glutathione (GSH). Dissolution behavior was evaluated in the ultra pure water (UPW), cell culture medium used for L929 cells (DMEM) and medium used for cultivation of *Daphnia magna* (SCM) after 24 h.

Particle	d_H [nm] (% mean volume)	ζ potential [mV[	% free metal ions		
			UPW	DMEM	SCM
CYS AuNPs	10.6 ± 2.4 (41%) 36.3 ± 8.6 (59%)	-46.8 ± 2.1	No dissolution!		
CYS AgNPs	8.0 ± 0.9 (100%)	-56.9 ± 7.5	0,13	0,22	0,26

GSH AuNPs	7.4 ± 2.1 (38%)	-58.0 ± 3.8	No dissolution!		
	65.1 ± 13.8 (62%)				
GSH AgNPs	6.0 ± 1.2 (100%)	-50.9 ± 2.3	0,10	0,77	0,64

As the biological effect metallic NPs may originate from the release of metallic ions in biological environment, it was important to evaluate dissolution behavior of NPs. Release of Ag^{+} and Au^{3+} ions from AgNPs and AuNPs surfaces was studied in UPW and media relevant for biological experiments, *i.e.* EMEM + 10% FBS used as a culture media for fibroblasts and standard culture media (SCM) used for *D. magna*. As expected, AuNPs did not dissolved in any of tested media, while both CYS- and GSH-coated AgNPs released more ions in media used for biological experiments (EMEM + 10% FBS and SCM) compared to the UPW (**Table 1**). However, the amount of free Ag^{+} measured after incubation of AgNPs in these media did not exceed 1%. This does not necessarily mean that Ag^{+} release is negligible, since underestimation of ionic Ag could happen due to complexes formed with component of tested which can precipitate or cannot pass the filter.

Biocompatibility assessment

Effect of CYS- and GSH-coated AgNPs or AuNPs on mammalian cells *in vitro* was investigated to determine biocompatibility of biothiol-functionalized NPs. For this purpose, efficiency of NPs uptake, cell viability, mechanism of cell death oxidative stress response and genotoxicity parameters of L292 cells treated with NPs were determined and compared with control cells.

A range of NPs concentrations were tested for negative effects on the survival and viability of L929 cells after 24 h exposure. For comparative purposes, cells were also treated with different concentrations of Ag^{+} (in the form of $AgNO_3$) and Au^{3+} (applied as $HAuCl_4$). The results, as presented in **Figure 4**, demonstrated dose-dependent toxic effects of CYS- and GSH-coated AgNPs, while

AuNPs showed no toxicity in the tested concentration range (1 – 300 mg Au L^{-1}). Only GSH-coated AgNPs decreased cell viability by 20% at the dose of 300 mg Au L^{-1}. The GSH-coated AgNPs decreased cell viability by more than 50% at dose 5 times lower than CYS-coated AgNPs. Ionic silver was the most toxic and destroyed the cells at 10 times higher dose compared to Au^{3+} (**Figure 4a**).

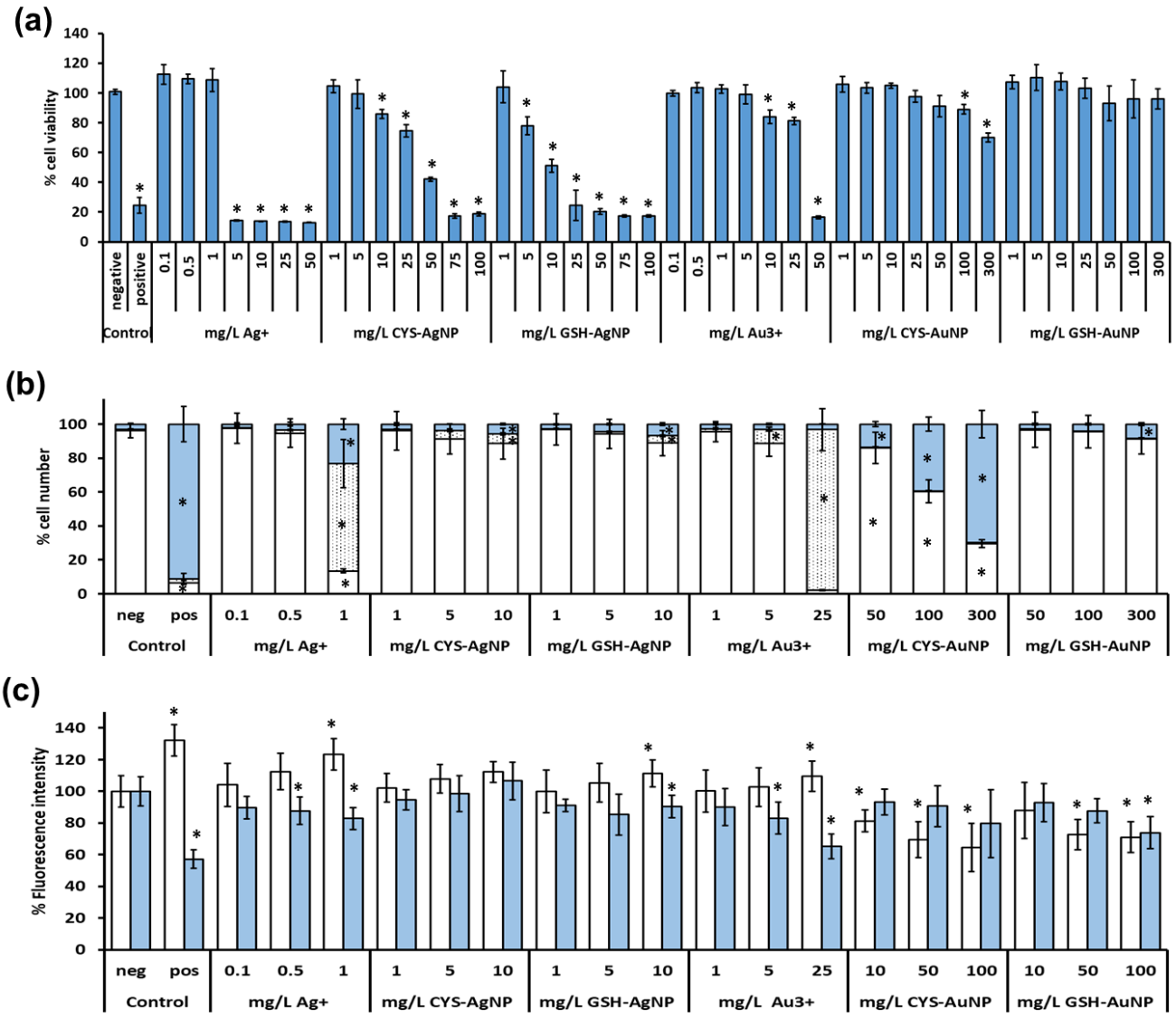

Figure 4. (a) Viability of L929 cells exposed to silver (AgNPs) and gold nanoparticles (AuNPs) stabilized with cysteine (CYS) or glutathione (GSH), Ag^{+} and Au^{3+} ions during 24 h and determined by the MTT cytotoxicity assay. (b) The effect of AgNPs, AuNPs, Ag^{+}, and Au^{3+} on the number of live (white columns), early apoptotic (doted columns) and late apoptotic (blue columns) L929 cells after

24h exposure, determined by flow cytometry after Annexin V/PI staining. (c) The effect of AgNPs, AuNPs, Ag^{+}, and Au^{3+} on the level of peroxy radical (white columns, as measured by DCFH-DA assay) and total GSH (blue columns, as measured by MBCl assay) in L929 cells after 4 h of exposure. Negative controls (neg) were untreated cells. Positive controls (pos) were cells treated with DMSO for MTT and Annexin V/PI assays, or with the *t*-butylhydroxyde for DCFH and MBCl assays. Results are expressed as percentage of negative controls and given as mean values obtained from 3 independent experiments. Standard deviations are presented as scale bars. Values marked with asterisk (*) differ significantly from the negative control ($P < 0.05$).

Evidently, the most lethal tested substance was Ag^{+} followed by GSH-coated AgNPs. If we compare this results with data published on polymer-coated NPs on the same cell type, toxicity of GSH-AgNPs is similar to effect of polyvinylpyrrolidone (PVP) stabilized AgNPs reported earlier,[68] while another study found > 90% live L929) cells after 24 h treatment with commercial PVP-coated AgNPs.[69] Our results on AuNPs effects corroborate well with similar study on L929 cells treated with PVP-coated AuNPs.[70]

Further biocompatibility testings were performed using concentration range of NPs or ions that did not cause decrease of cell viability by more than 80%. Uptake of AuNPs and AgNPs, as determined by flow cytometry, showed dose-dependent cell penetration of all NPs (**Figure S6 in SI**). The highest efficiency of cell uptake was observed for CYS-coated AuNPs. For both CYS- and GSH-coated AgNPs, the uptake is significant only at the highest examined concentration (25 mg Ag L^{-1}). The behavior of GSH AuNPs deviates considerably from the others and did not show any significant change in the SSC ratio even at the highest dose applied indicating no cell accumulation. Given the likenesses in shape, size and charge of all NPs, analogous uptake profiles were expected and these results represent an anomaly.

To gain closer insight into the mechanisms of toxic actions of silver and gold NPs and ions, percentage of live, early apoptotic and late apoptotic/dead cells were determined by staining with CAM and EthD dyes and flow cytometry analysis. Doses that caused low or no death of fibroblasts, showed apoptotic processes in a dose-response manner for all tested species (**Figure 4b**). In accordance with the MTT data (**Figure 4a**), ionic species at the highest concentration applied, i.e. 1 mg Ag L^{-1} and 25 mg Au L^{-1}, triggered apoptosis in 86% and 95% of cells, respectively. Silver and gold NPs were biocompatible inducing at tested doses less than 20% of apoptotic events (**Figure 4b**). Only treatment with GSH-AuNPs led to significant number of late apoptotic cells. Interestingly, CYS- and GSH-coated AgNPs were shown to be safer than expected. In both cases, more than 88% of fibroblasts survived the treatment with the highest dose applied (10 mg Ag L^{-1}).

As exposure to NPs is known to induce oxidative stress in cells,[71,72] ROS production and intracellular GSH level were measured after 24 h incubation with tested species. Results corroborated well with those on the number of apoptotic cells. In all cases where doses of tested induced apoptosis in fibroblasts, ROS levels were also significantly changed (**Figure 4c**). Interestingly, AgNPs and ionic form of metals increased, while AuNPs decreased significantly the amount of ROS possibly due to the activation of protective mechanisms against oxidative stress.[73] Previous study on human pulmonary fibroblasts also found that AuNPs cause higher oxidative stress than AgNPs.[74] Level of GSH changed significantly compared to controls only in cases where number of apoptotic cells where higher than 40%, i.e. cells treated with Au^{3+} or Ag^{+}. Once more, NPs were proven less toxic than their ionic counterparts, requiring 10 – 50 times higher doses to achieve the same toxic effect.

As oxidative stress may induce damages to DNA molecules,[75] which will consequently lead to apoptosis if severe enough, the DNA damage signaling pathway was evaluated by detecting the ATM and H2A.X activated cells, as well as their dual activation which indicates DNA double-strand breaks. DNA double-strand breaks may lead to chromosome aberrations, genomic instability, or cell death.[76]

Evaluation of ATM and H2A.X activation is more accurate and quantitative measurement of DNA damage response at the single cell level. The total percentage of damaged cells is a sum of ATM positive, H2.X positive and double-positive cells. Although, the number of cells positive for DNA damage was low (**Figure 5**), clear dose-dependent activation for each target was observed. In the case of ionic forms, the number of cells with DNA damages increased with the increase of Au^{3+} or Ag^{+} concentration, while opposite trends were observed in cells treated with NP (**Figure 5**).

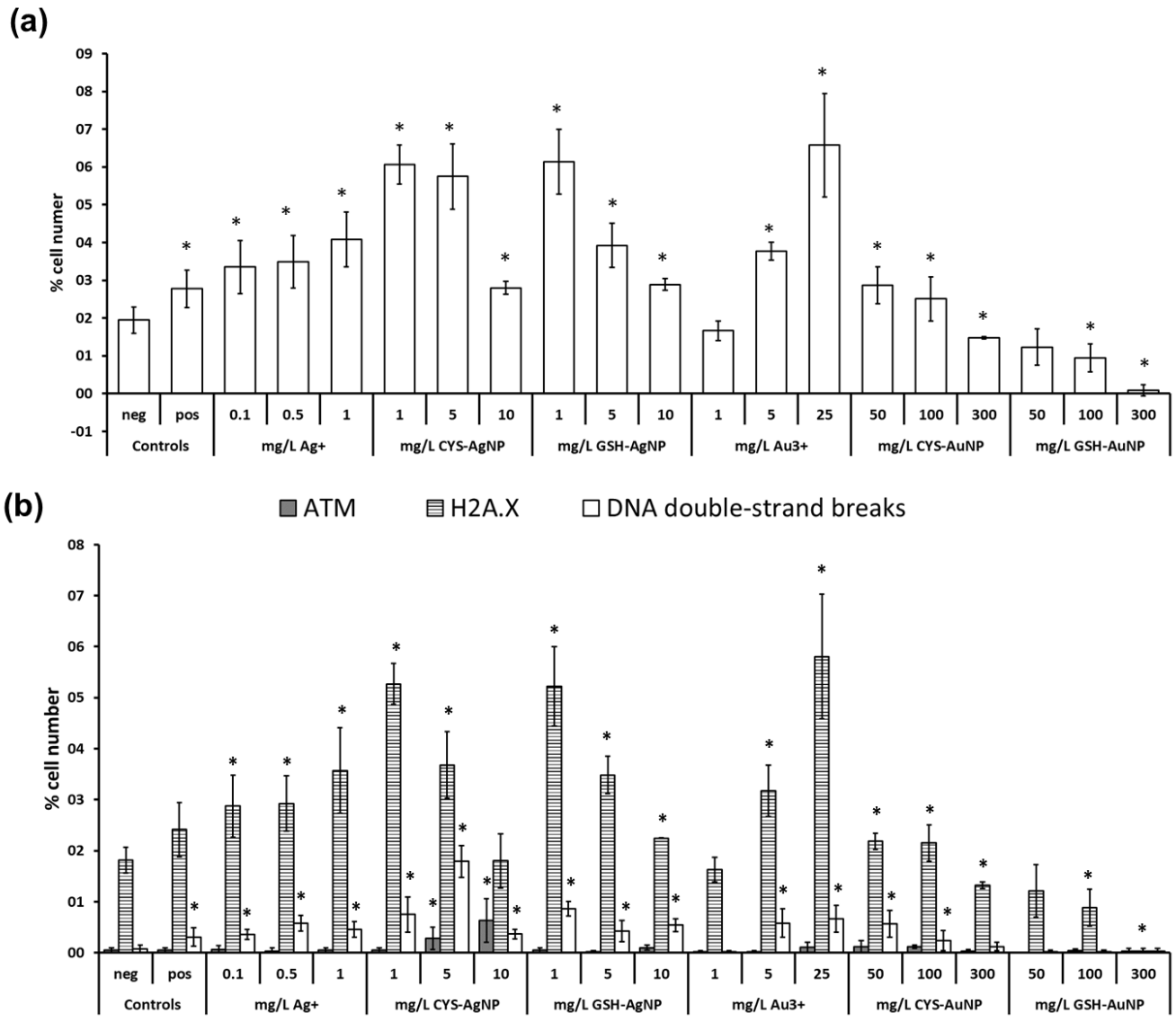

Figure 5. The effect of silver (AgNPs) and gold nanoparticles (AuNPs) stabilized with cysteine (CYS) or glutathione (GSH), Ag^{+} and Au^{3+} ions on (a) total DNA damage and (b) DNA double-stranded breaks (white columns), the activation of ATM (grey columns) and H2A.X (striped columns) in L929 cells after 24h exposure, measured with Muse™ Multi-Color DNA Damage Kit. Negative controls (Neg) were untreated cells, while positive controls (pos) were cells treated with DMSO. Results are expressed as percentage of negative controls and given as mean values obtained from 3 independent experiments. Standard deviations are presented as scale bars. Values marked with asterisk (*) differ significantly from the negative control ($P < 0.05$).

This could be the result of higher mortality of cells exposed to larger concentrations of AgNPs and AuNPs, lowering the overall number of cells with activated ATM and H2.X. It is important to note that the total percentage of cells with DNA damage stays below 7% in all of the cases. Thus, the overall harmful effect of AgNPs and AuNPs on DNA was relatively small for tested concentration range and duration of exposure (24 h), as evidenced also by evaluation of apoptosis and oxidative stress response. In general, ionic forms were the most toxic, following AgNPs, while AuNPs can be considered safe to cells. With regard to the effects of the coating, the results are inconclusive. The GSH-AgNPs decreased cell viability at lower concentration than CYS-AgNPs, but there were no significant differences between these two treatment for induction of apoptosis, DNA damage or oxidative stress response. In the case of AuNPs, CYS-AuNPs were slightly more toxic than GSH-AgNPs with regard to cell viability, the number of cells in late apoptosis, and DNA damages. This can be explained with more efficient internalization of these type of AuNPs (**Figure S6 in SI**). The GSH-AuNPs showed not just as less toxic than CYS-AuNPs, but even demonstrated lower activation of ATM and H2.X than in control cells.

When comparing toxicity of CYS- or GSH-coated AuNPs and AgNPs with NPs of the same core shell (Au or Ag) but with other type of stabilization agents, it may be concluded that CYS-AuNPs and GSH-AuNPs demonstrated low or even no toxicity as other types of AuNPs,[70] toxicity of CYS-AgNPs was similar to other types of AgNPs,[68] while GSH-AgNPs demonstrated as the most toxic type of AgNPs. This comparison took into account only results published on L929 cell line.

Acute toxicity test on *D. magna*

Ecotoxicological impact of CYS- and GSH-coated AuNPs and AgNPs was tested using aquatic crustacean *D. magna* Straus as model organism due to its ecological significance and widespread use in regulatory testing.[77] Acute toxicity tests were performed after 24 h and 48 h of exposure to NPs, while treatment with Ag^{+} and Au^{3+} was included for comparative purposes (**Table 2**).

Table 2. Acute toxicity of ionic silver and gold, silver (AgNPs) and gold nanoparticles (AuNPs) stabilized with cysteine (CYS) or glutathione (GSH), to *Daphnia magna* Straus. EC_{50} values, no adverse observed adverse effect (NOAEL) and lowest observed adverse effect levels (LOAEL) are given in µg Ag or Au L^{-1} and expressed as mean values obtained from 6 experiments and include standard deviations (SD), while 95% confidence intervals (CI) are given in parentheses.

Species examined	EC_{50} (95% CI)		NOAEL		LOAEL	
	24h	48 h	24h	48 h	24h	48 h
CYS-AgNP	347.6 ± 5.39 (344.19 - 364.39)	193.1 ± 5.20 (192.73 - 206.39)	50	20	100	50
GSH-AgNP	152.5 ± 6.20 (150.76 - 166.14)	119.0 ± 5.79 (116.92 - 131.31)	50	12	75	50

CYS-AuNP	/	/	2500	250	5000	500
GSH-AuNP	/	/	75	25	100	50
Ag^{+}	1.06 ± 5.69	0.97 ± 5.13	0.1	<0.1	0.5	0.1
	(0 - 12.75)	(0 - 11.74)				
Au^{3+}	12.7 ± 6.23	10.4 ± 6.19	5	4	7	5
	(12.15 - 27.61)	(8.63 - 24.01)				

Obtained values for EC_{50}, NOAEL and LOAEL values demonstrated significantly higher toxicity of Ag^{+} and Au^{3+} compared to AgNPs. It was not possible to determine EC_{50} value for AuNPs, as NOAEL and LOAEL values reached g L^{-1} levels for both CYS- and GSH-coated AuNPs. The CYS-AgNPs was slightly less toxic to *D. magna* than GSH-AgNPs. Indeed, trend for toxicity potential of tested ionic and nanoparticulate forms of Au and Ag were similar for aquatic organism as for mammalian cells. However, concentrations that caused harmful effects were much lower in aquatic toxicity tests.

Microscopic evaluation of treated and survived *D. magna* was performed additionally to assess if any accumulated NPs can be found in digestive tract of these animals. Deposits of NPs, but also of ingested ionic Ag, were visible as black dots (**Figure 6**). No traces of Au^{3+} were found. These micrographs evidenced that *D. magna* was exposed to NPs through digestion. Such results manifest harmful environmental effects of metallic NPs as already evidenced in earlier studies.[78–80]

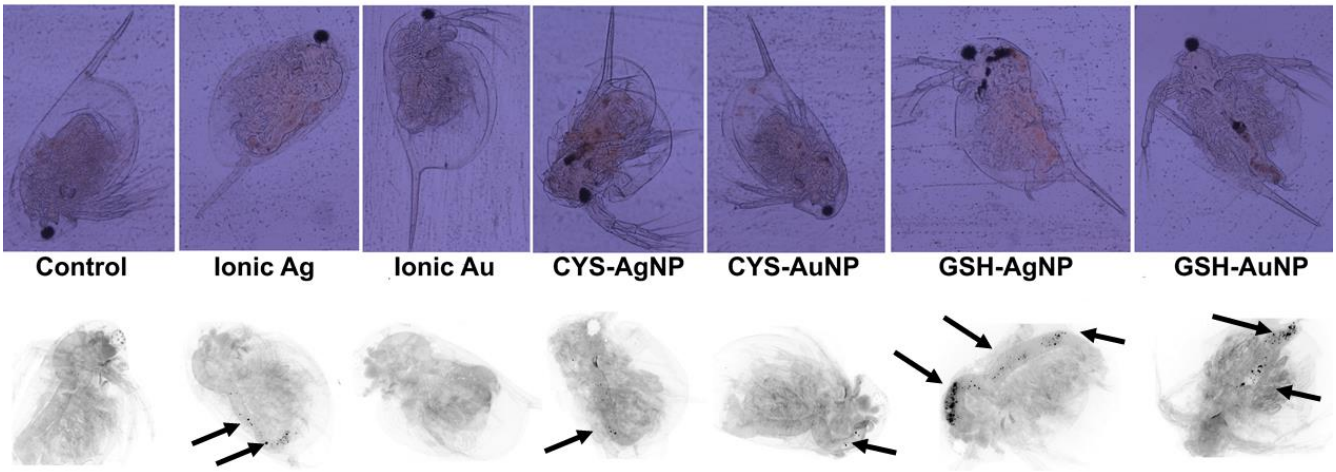

Figure 6. Micrographs of *D. magna* neonates after 48h exposure to ionic and nanoparticulate forms of Ag and Au. Visible accumulation is marked with arrows.

Interestingly, comparison of these results with previously published toxicity data indicated that CYS- or GSH-coated AgNPs and AuNPs were much less toxic to *D. magna* than polymer- or citrate-coated AgNPs and AuNPs (see Table S2 in Supporting Material). This trend is completely opposite to effects observed for mammalian cells *in vitro*.

CONCLUSION

As the interest in metallic nanoparticles for biomedical uses grows, the need emerges for the development of safe and biocompatible surface-modified nanosystems. For the first time, safety profiling of AgNPs and AuNPs prepared by using cysteine and glutathione as stabilizing agents was performed. Careful and comprehensive evaluation of physico-chemical properties and surface modification of these NPs revealed stabilization of both AgNPs and AuNPs occurred through interaction of metallic nanosurface with disulfide of oxidized forms of cysteine and glutathione. This important observation sheds new light on the mechanism of NPs formation in the presence of thiols.

Assessment of NPs toxicity on mammalian cells in vitro and aquatic organism in vivo evidenced that surface modification of metallic NPs with biothiols made them safer for the environment, but more toxic for use in humans. Further studies should be directed toward transformation patterns of NPs in vivo and the role of nano-bio interactions that may either lead to less or more toxic transformed nanospecies.

MATERIALS AND METHODS

Chemicals and reagents

All chemicals used were purchased from Sigma Aldrich (Darmstadt, Germany) unless stated otherwise. Silver nitrate ($AgNO_3$) was purchased from Alfa Aesar (Karlsruhe, Germany). All compounds were reagent-grade or higher.

Synthesis and characterization of AgNPs and AuNPs in the presence of CYS and GSH

AgNPs and AuNPs were synthesized by the reduction of silver and gold salts, respectively, using sodium borohydride in the presence of CYS or GSH as stabilizing agents. Several synthetic approaches were tested, where different experimental parameters (concentration and ratio of reactants, ordering of reactants addition, mixing time and speed, etc.) as presented in Tables S1-S2 given in Supporting Materials. All synthesis were performed at room temperature and the mixtures were protected from light. Obtained NPs were carefully characterized by means of size distribution and surface charge employing dynamic (DLS) and electrophoretic light scattering (ELS) methods. Visualization of NPs was performed using transmission electron microscopy (TEM). The most stable AuNPs and AgNPs with similar physico-chemical properties were obtained by procedure in which appropriate amounts of $HAuCl_4$ or $AgNO_3$ were dissolved in ultrapure water (UPW). Solutions of biothiols (CYS or GSH) were then added and left to stir for 10 min. Finally, $NaBH_4$ was added dropwise under vigorous

stirring. The mixture was left to react for 2 h. The molar ratio of [metallic salt] : [reducens] : [biothiol] = 1 : 10 : 1 was chosen. For AuNPs, the final concentrations of reagents were 3 mM $HAuCl_4$, 30 mM $NaBH_4$ and 3 mM biothiol, while 5.6 mM $AgNO_3$, 56 mM $NaBH_4$ and 5.6 mM biothiol were employed for AgNPs. After synthesis, each NPs were washed twice with UPW using ultracentrifugation at 15000 x g for 40 min. Washed NPs were kept in the dark at 4 °C.

The concentrations of AgNPs and AuNPs were determined as total Ag and Au content, respectively, analyzed by Agilent Technologies 7800 inductively coupled plasma mass spectrometer (ICPMS) (Agilent, Waldbronn, Germany). Visualization was performed using TEM 902A instrument (Carl Zeiss Meditec AG, Jena, Germany). The microscope operated in the bright-field mode and the acceleration voltage at 80 kV. TEM samples were prepared on a Formvar®-coated copper grid by depositing a drop of the particle suspension and leaving to air-dry at room temperature. Images were recorded with an attached Canon PowerShot S50 camera. Both DLS and ELS measurements were performed at room temperature using Zetasizer Nano ZS (Malvern Instruments, Malvern, UK) with a green laser (532 nm), set at an angle of 173 °. Size distributions of NPs are expressed as hydrodynamic diameter (d_H) obtained from the size-volume distribution function and given as an average of 10 measurements. Surface charge was determined by measuring the electrophoretic mobility, which was converted to zeta (ζ) potential values using the Henry equation with the Smoluchowski approximation. The measurements were repeated 5 times. DLS and ELS data processing was performed using Zetasizer software 6.32 (Malvern Instruments).

Dissolution behavior of AuNPs and AgNPs was tested by ultrafiltration followed by quantification of released free gold or silver ions. The test media were UPW, cell culture medium EMEM with the addition of 10% FBS and standard culture media for *Daphnia magna* cultivation (SCM). Freshly prepared NPs were diluted in the test media to a final concentration of 10 mg L^{-1}, left stirring in the dark for 1 h following filtration using Amicon-4 Ultra centrifugal filter units of 3 kDa cut-off size

(Merck Millipore, Darmstadt, Germany). Obtained filtrates were immediately acidified with HNO_3 to a final acid content of 10% (v/v). Released silver or gold ions were quantified by ICP-MS. The reliability of the employed analytical method was confirmed using the Standard Reference Material® (SRM) 1643e Trace Elements in Water (NIST, USA). The results are presented as average values of 5 independent measurements.

NMR experiments

Progress of the reaction in the mixture of biothiols, metallic salts, and/or $NaBH_4$, was followed by ^{1}H and ^{13}C nuclear magnetic resonance (NMR) spectroscopy using the Varian INOVA 400 spectrometer operating at 399.6 and 99.9 MHz, respectively. Samples were prepared in UPW with the addition of D_2O to a final volume ratio of 10%, or, in some cases, a capillary filled with D_2O was used as an external lock. ^{1}H NMR spectra were recorded in 10-20 min intervals during NPs synthesis, starting immediately after the mixing of reagents (t0). Chemical shifts were expressed in parts per million (ppm) and are referenced to the residual water signal. All spectra were recorded at 25 ◦C. For all experiments, a recycle delay of 5 s was used, which was sufficiently greater that the relaxation time T_1. To suppress the solvent signal the WET and PRESAT pulse sequences were used, as available in VnmrJ (4.2A) software.

Cell experiments

Murine fibroblast (L929) cells were cultured in EMEM with addition of FBS (10%) and Penicillin/Streptomycin (1%) in a T25 culture flask (Eppendorf, Germany). When cells reached 80% confluence, culture medium was removed with pipette; cells were washed once with sterile phosphate buffer saline (PBS), detached from the flask by adding Trypsin-EDTA (0.25%) solution and incubated for 10 min at 37 °C and 5% CO_2. Detached cells were collected, counted on TC20 automated cell

counter (Biorad, USA), seeded in sterile 96-well plates or 12-well plates (Eppendorf, Germany) for subsequent treatment. Seeded cells growth for 24 h at 37 °C and 5% CO_2 to allow cell attachment. The following day, AgNPs, AuNPs, $AgNO_3$ and $HAuCl_4$ were added to wells in different concentrations and treated for 24 hours.

The MTT assay, based on the reduction of the yellow tetrazolium salt MTT (3-(4,5-dimethylthiazol-2-yl)-2,5-diphenyltetrazoliumbromide) to a purple MTT-formazan crystal by metabolically active cells, was used to determine cell viability after 24-hour exposure. The assay was performed according to manufacturer's instruction. Briefly, the cells were seeded in 96-well tissue culture plates (5×10^4 cells/ml growth medium) followed by an overnight incubation. Different concentrations of NPs or salt suspensions were added (to a final concentration range of 1 – 100 mg L^{-1} for AgNPs, 1 – 300 mg L^{-1} for AuNPs) and left to incubate for 24 h. For the purpose of comparison, the cells were also incubated with $AgNO_3$ and $HAuCl_4$, in the final concentration ranges of 0.1 – 50 mg L^{-1}. Untreated cells were used as negative controls, while the cells treated with dimethyl sulfoxide (DMSO) (10% (v/v)) were used as positive controls. After incubation, the medium was removed from the wells by aspiration; the cells were washed 3 times with PBS (200 µL per well) and of MTT solution (50 µL, 1000 mg L^{-1}) was added to each well. The dye was left to incubate for 4 h at 37 °C, after which the MTT solution was removed by aspiration. Remaining formazan crystals were dissolved by addition of DMSO (50 µL) and shaking the plates. The absorbance was recorded at 530 nm using a Victor™ multilabel reader (Perkin Elmer, Massachusetts, USA).

The ratio of live, apoptotic and dead cells after treatment with NPs or respective metal salts was determined by flow cytometry experiments using Annexin V and propidium iodide staining. Annexin V binds phosphatidylserine, which can only be found on the outer leaflet of cell membranes during apoptosis. Propidium iodide is a DNA-binding agent that cannot penetrate the membrane of living cells, and thus can only stain dead or late apoptotic ones. The treatment involved 24 h incubation with

AgNPs (ranging between 1 – 10 mg Ag L^{-1}), AuNPs (50 – 300 mg Au L^{-1}), $AgNO_3$ (0.1 – 1 mg Ag L^{-1}) and $HAuCl_4$ (1 – 25 mg Au L^{-1}). Positive controls were cells treated with paraformaldehyde (0.04 mg L^{-1}), while untreated cells were negative controls. After treatment, the plates were centrifuged at 1500 × *g* for 15 min. Supernatants containing dead cells were collected from 12-well plate in 1.5 mL Eppendorf tubes. Live cells were detached from wells by adding 0.05 % GibcoTM Trypsin-EDTA (Thermo Fisher Scientific, Waltham, U.S.) solution, washed with PBS, resuspended in PBS-based buffer containing FBS (2%) and EDTA (2 mmol L^{-1}) (pH 7.4, filtered through 0,2 μm sterile filter) and passed through a 40 μm Falcon™ cell strainer (Thermo Fisher Scientific). Supernatants and the detached cells were joined, centrifuged at 800 x *g* for 5 minutes and washed with PBS containing 2% bovine serum albumin (1 mL per sample). Cells were stained using Muse® Annexin V and Dead Cell Assay Kit (Merck KGaA, Darmstadt, Germany) according to manufacturer's instructions. After staining, cells were washed twice by adding PBS (1 mL per sample) and analyzed using Muse™ Cell Analyzer along with the corresponding Muse™ software module. Data are expressed as % relative to negative controls.

Internalization of NPs was evaluated using Molecular Probes™ LIVE/DEAD™ kit (Invitrogen, Fisher Scientific) Attune® acoustic focusing flow cytometer (Applied Biosystems, USA) equipped with a 488 nm laser. For the experiment, L929 cells were seeded in 6-well plates at a density 2.5×10^5 cells/well. After 48 hours, the culture medium was exchanged with a fresh one and increasing concentrations of AgNPs (1, 5 or 25 mg Ag L^{-1}) or AuNPs (25, 50 or 100 mg Au L^{-1}) were added. Negative control were non-treated cells. Dissociated cells were incubated with calcein acetoxymethyl ester (CAM)(0.1 μM) and ethidium homodimer-1 (EthD)(3 μM), both supplied in the kit, for 15 min in the dark at room temperature. Each experiment was repeated at least 3 times. CAM and EthD were measured using log amplifiers. The percentage of NPs-labelled cells was determined using Attune acoustic focusing cytometer by measuring the increase of the side scattered light of the laser beam (SSC). The intensity

of the SSC is proportional to the intracellular density and granularity.[81] As NPs uptake increases the intracellular density, the SSC intensity is also enhanced. Results were analyzed by FCS Express 5 Flow Cytometry Software using Overton cumulative histogram subtraction method.[82]

Reactive oxygen species (ROS) production in cells treated with AgNPs and AuNPs was determined by the 2′,7′-dichlorodihydrofluorescein diacetate (DCFH-DA) staining. DCFH-DA is a non-fluorescent dye that can freely permeate cell membranes. Inside the cell, it is hydrolyzed by cellular esterases to form DCFH, which is then oxidized by intracellular ROS to fluorescent 2′,7′-dichlorofluorescein (DCF). After treatment of L929 cells with AgNPs (in concentration range 1 – 5 mg Ag L^{-1}), AuNPs (10 – 100 mg Au L^{-1}), $AgNO_3$ (0.1 – 1 mg Ag L^{-1}) and $HAuCl_4$ (1 – 25 mg Au L^{-1}) for 4 h at 37 °C, the cells were washed three times with PBS and stained with DCFH-DA (20 μM) for 30 minutes at 37 °C. Then, cells were washed again with PBS two times and analyzed using a Victor™ multilabel reader (Perkin Elmer, MA) at an excitation wavelength of 485 nm and emission wavelength of 535 nm. Untreated cells were used as negative controls, while cells treated with hydrogen peroxide (100 μM) served as positive controls. Data are expressed as percentage of fluorescence intensity compared to negative controls.

The changes in the intracellular level of GSH were measured using monochlorobimane (MBCl) staining. This fluorogenic bimane probe forms a fluorescent adduct with GSH.[83] The treatment of cells was performed following the same protocol as for the DCFH-DA assay, and the same controls were used. After treatment, the cells were washed thrice with PBS, incubated with MBCl (50 μM) for 20 minutes at 37 °C, washed again twice with PBS and analyzed using a Victor™ multilabel reader at an excitation wavelength of 355 nm and emission wavelength of 460 nm. Data are expressed as percentage of fluorescence intensity compared to negative controls.

DNA damage in L9292 cells was assessed using the Muse™ Multi-Color DNA Damage Kit (EMD Millipore) according to manufacturer's instructions. The kit measures the activation of Ataxia

telangiectasia mutated kinase (ATM) and Histone H2A.X by phosphorylation, using a phospho-specific ATM (Ser1981)-PE and a phospho-specific Histone H2AX-PECy5 conjugated antibodies. This kit simultaneously provides statistical data for each of two critical DNA damage markers at the single-cell level. The percentages of negative (undamaged) cells, ATM activated cells, H2AX activated cells and DNA double-strand breaks (dual activation of both ATM and H2AX) were counted on the Muse™ Cell Analyzer along with the corresponding Muse™ software module.

Each cell experiment was repeated at least 3 times.

Acute toxicity test on Daphnia magna

Acute ecotoxicity tests were performed on *D. magna* Straus, an aquatic model organism for ecotoxicity testings. *D. magna* Straus clone MBP996 was purchased as Toxkit Ephippia (MicroBio-Tests Inc., Mariakerke, Belgium). Dormant eggs (ephippia) were incubated in standard culture media (SCM) prepared as reconstituted hard water with the addition of $CaCl_2 \times 2H_2O$ (294 mg L^{-1}), $MgSO_4 \times 7H_2O$ (123.25 mg L^{-1}), $NaHCO_3$ (64.75 mg L^{-1}), and KCl (5.75 mg L^{-1}) at pH 7.8 ± 0.5, without any organic compounds. HRN EN ISO 6341:2013 protocol and Toxkit Ephippia supplier instruction for handling were followed. The exposure was carried out in the dark and the temperature was maintained between 19 and 21 °C.

Concentrated stock solutions AgNPs, AuNPs, $AgNO_3$ and $HAuCl_4$ were diluted in the SCM to concentrations ranging between 5-1000 mg Ag L^{-1}, 5-5000 mg Au L^{-1}, 0.1-10 mg Ag L^{-1} and 0.5-50 mg Au L^{-1}, respectively. Properties of SCM such as temperature, pH, conductivity and oxygen levels were assessed using the respective probes from Orion Research Inc. (USA), at the start and end of the experiment. Groups of 5 *D. magna* neonates (24 hours old) were transferred into glass test vessels that contained 10 mL of SCM (control) or tested compounds diluted in the SCM. Great care was taken during the transfer to avoid hurting any daphnids, which would lead to false conclusions. Daphnids

were incubated for 24 and 48 hours without feeding during treatment period. The tests were performed four times each in four replicates. Mortality of *D. magna* was the endpoint of the test. The acute toxicity was expressed as EC_{50}, effective concentration that causes mortality of 50% daphnids) with 95% confidence intervals (CI). No observable adverse effect level (NOAEL), and lowest observable adverse effect level (LOAEL) were also recorded. In addition, surviving and normal daphnids were inspected by light microscopy to visualize accumulation of Ag or Au in gut. After 48h treatment, daphnids were washed with PB pH 7.4 and put on microscopic glass using cover slip mounted in Vectashield (Vector Laboratories, Burlingame, CA). Opton III RS fluorescence microscope (Opton Feintechnik, Oberkochen, Germany) with x10 magnification was used for examination and the images were recorded with a Spot RT Slider camera (Diagnostic Instruments, Sterling Heights, MI). Image processing was performed in Adobe Photoshop 6.0.

Statistical analysis

Statistical analysis was carried out using Dell™ Statistica™ 13.2 software (StatSoft, Tulsa, USA). Data represent mean values and standard deviations (SD). Differences between treatments for the different measured variables were tested using simple and repeated measures ANOVA, followed by Fisher LSD *post-hoc* test when significant differences were found ($P < 0.05$). The homogeneity of variances was tested using the Levene test. The level of significance ($P < 0.05$) is indicated by the asterisks (*) for differences between treatments and controls.

Supporting Information

Supporting Information are available online.

Acknowledgements

The Croatian Science Foundation (grant number IP-2016-06-2436) is acknowledged for financial support.

References

[1] B. Pelaz, C. Alexiou, R. A. Alvarez-Puebla, F. Alves, A. M. Andrews, S. Ashraf, L. P. Balogh, L. Ballerini, A. Bestetti, C. Brendel, S. Bosi, M. Carril, W. C. W. Chan, C. Chen, X. Chen, X. Chen, Z. Cheng, D. Cui, J. Du, C. Dullin, A. Escudero, N. Feliu, M. Gao, M. George, Y. Gogotsi, A. Grünweller, Z. Gu, N. J. Halas, N. Hampp, R. K. Hartmann, M. C. Hersam, P. Hunziker, J. Jian, X. Jiang, P. Jungebluth, P. Kadhiresan, K. Kataoka, A. Khademhosseini, J. Kopeček, N. A. Kotov, H. F. Krug, D. S. Lee, C.-M. Lehr, K. W. Leong, X.-J. Liang, M. Ling Lim, L. M. Liz-Marzán, X. Ma, P. Macchiarini, H. Meng, H. Möhwald, P. Mulvaney, A. E. Nel, S. Nie, P. Nordlander, T. Okano, J. Oliveira, T. H. Park, R. M. Penner, M. Prato, V. Puntes, V. M. Rotello, A. Samarakoon, R. E. Schaak, Y. Shen, S. Sjöqvist, A. G. Skirtach, M. G. Soliman, M. M. Stevens, H.-W. Sung, B. Z. Tang, R. Tietze, B. N. Udugama, J. S. VanEpps, T. Weil, P. S. Weiss, I. Willner, Y. Wu, L. Yang, Z. Yue, Q. Zhang, Q. Zhang, X.-E. Zhang, Y. Zhao, X. Zhou, W. J. Parak, *ACS Nano* **2017**, *11*, 2313.

[2] S. Aziz, S. Aziz, A. Akbarzadeh, *Drug Res. (Stuttg).* **2017**, *67*, 198.

[3] S. U. Khan, T. A. Saleh, A. Wahab, M. H. U. Khan, D. Khan, W. U. Khan, A. Rahim, S. Kamal, F. U. Khan, S. Fahad, *Int. J. Nanomedicine* **2018**, *13*, 733.

[4] L. A. Austin, M. A. Mackey, E. C. Dreaden, M. A. El-Sayed, *Arch. Toxicol.* **2014**, *88*, 1391.

[5] X. F. Zhang, Z. G. Liu, W. Shen, S. Gurunathan, *Int. J. Mol. Sci.* **2016**, *17*, 1534.

[6] M. Yamada, M. Foote, T. W. Prow, *Wiley Interdiscip. Rev. Nanomedicine Nanobiotechnology* **2015**, *7*, 428.

[7] D. McShan, P. C. Ray, H. Yu, *J. Food Drug Anal.* **2014**, *22*, 116.

[8] S. Kim, D. Y. Ryu, *J. Appl. Toxicol.* **2013**, *33*, 78.

[9] C. A. Dos Santos, M. M. Seckler, A. P. Ingle, I. Gupta, S. Galdiero, M. Galdiero, A. Gade, M. Rai, *J. Pharm. Sci.* **2014**, *103*, 1931.

[10] R. J. Griffitt, J. Luo, J. Gao, J.-C. Bonzongo, D. S. Barber, *Environ. Toxicol. Chem.* **2008**, *27*, 1972.

[11] S.-Y. Park, J.-H. Choi, *Environ. Eng. Res.* **2010**, *15*, 23.

[12] B. K. Gaiser, T. F. Fernandes, M. A. Jepson, J. R. Lead, C. R. Tyler, M. Baalousha, A. Biswas, G. J. Britton, P. A. Cole, B. D. Johnston, Y. Ju-Nam, P. Rosenkranz, T. M. Scown, V. Stone, *Environ. Toxicol. Chem.* **2012**, *31*, 144.

[13] K. K. Panda, V. M. M. Achary, R. Krishnaveni, B. K. Padhi, S. N. Sarangi, S. N. Sahu, B. B. Panda, *Toxicol. Vitr.* **2011**, *25*, 1097.

[14] L. K. Limbach, P. Wick, P. Manser, R. N. Grass, A. Bruinink, W. J. Stark, *Environ. Sci. Technol.* **2007**, *41*, 4158.

[15] N. Lubick, *Environ. Sci. Technol.* **2008**, *42*, 8617.

[16] E. J. Park, J. Yi, Y. Kim, K. Choi, K. Park, *Toxicol. Vitr.* **2010**, *24*, 872.

[17] C. Batchelor-McAuley, K. Tschulik, C. C. M. Neumann, E. Laborda, R. G. Compton, *Int. J. Electrochem. Sci.* **2014**, *9*, 1132.

[18] K. Kawata, M. Osawa, S. Okabe, *Environ. Sci. Technol.* **2009**, *43*, 6046.

[19] S. Kim, J. E. Choi, J. Choi, K. H. Chung, K. Park, J. Yi, D. Y. Ryu, *Toxicol. Vitr.* **2009**, *23*, 1076.

[20] E. E. Connor, J. Mwamuka, A. Gole, C. J. Murphy, M. D. Wyatt, *Small* **2005**, *1*, 325.

[21] D. Tiedemann, U. Taylor, C. Rehbock, J. Jakobi, S. Klein, W. A. Kues, S. Barcikowski, D. Rath, *Analyst* **2014**, *139*, 931.

[22] J. Tournebize, A. Boudier, O. Joubert, H. Eidi, G. Bartosz, P. Maincent, P. Leroy, A. Sapin-Minet, *Int. J. Pharm.* **2012**, *438*, 107.

[23] M. A. Dobrovolskaia, S. E. McNeil, *Nat. Nanotechnol.* **2007**, *2*, 469.

[24] H. K. Patra, S. Banerjee, U. Chaudhuri, P. Lahiri, A. K. Dasgupta, *Nanomedicine Nanotechnology, Biol. Med.* **2007**, *3*, 111.

[25] G. Peng, U. Tisch, O. Adams, M. Hakim, N. Shehada, Y. Y. Broza, S. Billan, R. Abdah-Bortnyak, A. Kuten, H. Haick, *Nat. Nanotechnol.* **2009**, *4*, 669.

[26] C. Di Guglielmo, J. De Lapuente, C. Porredon, D. Ramos-López, J. Sendra, M. Borrás, *J. Nanosci. Nanotechnol.* **2012**, *12*, 6185.

[27] R. Shrivastava, P. Kushwaha, Y. C. Bhutia, S. J. S. Flora, *Toxicol. Ind. Health* **2016**, *32*, 1391.

[28] L. Truong, K. S. Saili, J. M. Miller, J. E. Hutchison, R. L. Tanguay, *Comp. Biochem. Physiol. - C Toxicol. Pharmacol.* **2012**, *155*, 269.

[29] Y. Pan, S. Neuss, A. Leifert, M. Fischler, F. Wen, U. Simon, G. Schmid, W. Brandau, W. Jahnen-Dechent, *Small* **2007**, *3*, 1941.

[30] X. D. Zhang, M. L. Guo, H. Y. Wu, Y. M. Sun, Y. Q. Ding, X. Feng, L. A. Zhang, *Int. J. Nanomedicine* **2009**, *4*, 165.

[31] J. H. Sung, J. H. Ji, J. D. Park, M. Y. Song, K. S. Song, H. R. Ryu, J. U. Yoon, K. S. Jeon, J. Jeong, B. S. Han, Y. H. Chung, H. K. Chang, J. H. Lee, D. W. Kim, B. J. Kelman, I. J. Yu, *Part. Fibre Toxicol.* **2011**, *8*, 1.

[32] D. Mateo, P. Morales, A. Ávalos, A. I. Haza, *J. Exp. Nanosci.* **2015**, *10*, 1401.

[33] Y. P. Jia, B. Y. Ma, X. W. Wei, Z. Y. Qian, *Chinese Chem. Lett.* **2017**, *28*, 691.

[34] R. de Lima, A. B. Seabra, N. Durán, *J. Appl. Toxicol.* **2012**, *32*, 867.

[35] M. F. Hornos Carneiro, F. Barbosa, *J. Toxicol. Environ. Heal. - Part B Crit. Rev.* **2016**, *19*, 129.

[36] C. Carnovale, G. Bryant, R. Shukla, V. Bansal, *Prog. Mater. Sci.* **2016**, *83*, 152.

[37] A. Gerber, M. Bundschuh, D. Klingelhofer, D. A. Groneberg, *J. Occup. Med. Toxicol.* **2013**, *8*, 1.

[38] I. Fratoddi, I. Venditti, C. Cametti, M. V. Russo, *Nano Res.* **2015**, *8*, 1771.

[39] M. Rösslein, J. T. Elliott, M. Salit, E. J. Petersen, C. Hirsch, H. F. Krug, P. Wick, *Chem. Res. Toxicol.* **2015**, *28*, 21.

[40] K. Park, E. J. Park, I. K. Chun, K. Choi, S. H. Lee, J. Yoon, B. C. Lee, *Arch. Pharm. Res.* **2011**, *34*, 153.

[41] V. A. Demin, I. V. Gmoshinsky, V. F. Demin, A. A. Anciferova, Y. P. Buzulukov, S. A. Khotimchenko, V. A. Tutelyan, *Nanotechnologies Russ.* **2015**, *10*, 288.

[42] S. Smulders, C. Larue, G. Sarret, H. Castillo-Michel, J. Vanoirbeek, P. H. M. Hoet, *Toxicol. Lett.* **2015**, *238*, 1.

[43] J. F. Hillyer, R. M. Albrecht, *J. Pharm. Sci.* **2001**, *90*, 1927.

[44] R. Wen, L. Hu, G. Qu, Q. Zhou, G. Jiang, *NanoImpact* **2016**, *2*, 18.

[45] M. van der Zande, R. J. Vandebriel, E. Van Doren, E. Kramer, Z. Herrera Rivera, C. S. Serrano-Rojero, E. R. Gremmer, J. Mast, R. J. B. Peters, P. C. H. Hollman, P. J. M. Hendriksen, H. J. P. Marvin, A. A. C. M. Peijnenburg, H. Bouwmeester, *ACS Nano* **2012**, *6*, 7427.

[46] C. A. Simpson, K. J. Salleng, D. E. Cliffel, D. L. Feldheim, *Nanomedicine Nanotechnology, Biol. Med.* **2013**, *9*, 257.

[47] G. Veronesi, C. Aude-Garcia, I. Kieffer, T. Gallon, P. Delangle, N. Herlin-Boime, T. Rabilloud, M. Carrière, *Nanoscale* **2015**, *7*, 7323.

[48] M. Marchioni, P. H. Jouneau, M. Chevallet, I. Michaud-Soret, A. Deniaud, *Coord. Chem. Rev.* **2018**, *364*, 118.

[49] C. Levard, B. C. Reinsch, F. M. Michel, C. Oumahi, G. V. Lowry, G. E. Brown Jr., *Environ. Sci. Technol.* **2011**, *45*, 5260.

[50] T. Miclăuş, C. Beer, J. Chevallier, C. Scavenius, V. E. Bochenkov, J. J. Enghild, D. S. Sutherland, *Nat. Commun.* **2016**, *7*, 1.

[51] A. Abraham, E. Mihaliuk, B. Kumar, J. Legleiter, T. Gullion, *J. Phys. Chem. C* **2010**, *114*, 18109.

[52] W. K. Paik, S. Eu, K. Lee, S. Chon, M. Kim, *Langmuir* **2000**, *16*, 10198.

[53] S. Aryal, B. K. C. Remant, N. Dharmaraj, N. Bhattarai, C. H. Kim, H. Y. Kim, *Spectrochim. Acta - Part A Mol. Biomol. Spectrosc.* **2006**, *63*, 160.

[54] T. G. Schaaff, G. Knight, M. N. Shafigullin, R. F. Borkman, R. L. Whetten, *J. Phys. Chem. B* **1998**, *102*, 9.

[55] N. W. H. Adams, J. R. Kramer, *Aquat. Geochemistry* **1999**, *5*, 1.

[56] E. Csapó, R. Patakfalvi, V. Hornok, L. T. Tóth, Á. Sipos, A. Szalai, M. Csete, I. Dékány, *Colloids Surfaces B Biointerfaces* **2012**, *98*, 43.

[57] F. Blaske, L. Stork, M. Sperling, U. Karst, *J. Nanoparticle Res.* **2013**, *15*, 1928.

[58] T. Udayabhaskararao, M. S. Bootharaju, T. Pradeep, *Nanoscale* **2013**, *5*, 9404.

[59] A. M. Smith, L. E. Marbella, K. A. Johnston, M. J. Hartmann, S. E. Crawford, L. M. Kozycz, D. S. Seferos, J. E. Millstone, *Anal. Chem.* **2015**, *87*, 2771.

[60] X. Liu, M. Yu, H. Kim, M. Mameli, F. Stellacci, *Nat. Commun.* **2012**, *3*, 1182.

[61] R. López-Cebral, M. Martín-Pastor, B. Seijo, A. Sanchez, *Prog. Nucl. Magn. Reson. Spectrosc.* **2014**, *79*, 1.

[62] Z. Ma, H. Han, *Colloids Surfaces A Physicochem. Eng. Asp.* **2008**, *317*, 229.

[63] J. A. Gardiner, J. W. Collat, *J. Am. Chem. Soc.* **1965**, *87*, 1692.

[64] R. E. Mesmer, W. L. Jolly, *Inorg. Chem.* **1962**, *1*, 608.

[65] R. Retnamma, A. Q. Novais, C. M. Rangel, L. Yu, M. A. Matthews, *Int. J. Hydrogen Energy* **2014**, *39*, 6567.

[66] A. Abraham, A. J. Ilott, J. Miller, T. Gullion, *J. Phys. Chem. B* **2012**, *116*, 7771.

[67] C. Jacobs, R. H. Müller, *Pharm. Res.* **2002**, *19*, 189.

[68] A. S. Takamiya, D. R. Monteiro, D. G. Bernabé, L. F. Gorup, E. R. Camargo, J. E. Gomes-Filho, S. H. P. Oliveira, D. B. Barbosa, *J. Endod.* **2016**, *42*, 953.

[69] L. Wei, J. Tang, Z. Zhang, Y. Chen, G. Zhou, T. Xi, *Biomed. Mater.* **2010**, *5*, 044103.

[70] M. Hashimoto, S. Yamaguchi, J. I. Sasaki, K. Kawai, H. Kawakami, Y. Iwasaki, S. Imazato, *Eur. J. Oral Sci.* **2016**, *124*, 68.

[71] I. Vinković Vrček, I. Žuntar, R. Petlevski, I. Pavičić, M. Dutour Sikirić, M. Ćurlin, W. Goessler, *Environ. Toxicol.* **2016**, *31*, 679.

[72] I. M. Pongrac, I. Pavicic, M. Milic, L. Brkic Ahmed, M. Babic, D. Horak, I. Vinkovic Vrcek, S. Gajovic, *Int. J. Nanomedicine* **2016**, *11*, 1701.

[73] W. Fan, X. Wang, M. Cui, D. Zhang, Y. Zhang, T. Yu, L. Guo, *Environ. Sci. Technol.* **2012**, *46*, 10255.

[74] A. Ávalos, A. I. Haza, D. Mateo, P. Morales, *Toxicol. Mech. Methods* **2015**, *25*, 287.

[75] B. J. Marquis, S. A. Love, K. L. Braun, C. L. Haynes, *Analyst* **2009**, *134*, 425.

[76] C. J. Bakkenist, M. B. Kastan, *Nature* **2003**, *421*, 499.

[77] A. Baun, N. B. Hartmann, K. Grieger, K. O. Kusk, *Ecotoxicology* **2008**, *17*, 387.

[78] F. Nasser, A. Davis, E. Valsami-Jones, I. Lynch, *Nanomaterials* **2016**, *6*, 222.

[79] G. A. Dominguez, S. E. Lohse, M. D. Torelli, C. J. Murphy, R. J. Hamers, G. Orr, R. D. Klaper, *Aquat. Toxicol.* **2015**, *162*, 1.

[80] L. Ulm, A. Krivohlavek, D. Jurašin, M. Ljubojević, G. Šinko, T. Crnković, I. Žuntar, S. Šikić, I. Vinković Vrček, *Environ. Sci. Pollut. Res.* **2015**, *22*, 19990.

[81] R. M. Zucker, K. M. Daniel, In *Nanoparticles in Biology and Medicine*; Soloviev, M., Ed.; Humana Press: Totowa, NJ, 2012; pp. 497–509.

[82] W. R. Overton, *Cytometry* **1988**, *9*, 619.

[83] D. Stevenson, D. Wokosin, J. Girkin, M. H. Grant, *Toxicol. Vitr.* **2002**, *16*, 609.